Biophysical Journal, Volume *118*

Supplemental Information

Microrheology for Hi-C Data Reveals the Spectrum of the Dynamic 3D Genome Organization

Soya Shinkai, Takeshi Sugawara, Hisashi Miura, Ichiro Hiratani, and Shuichi Onami

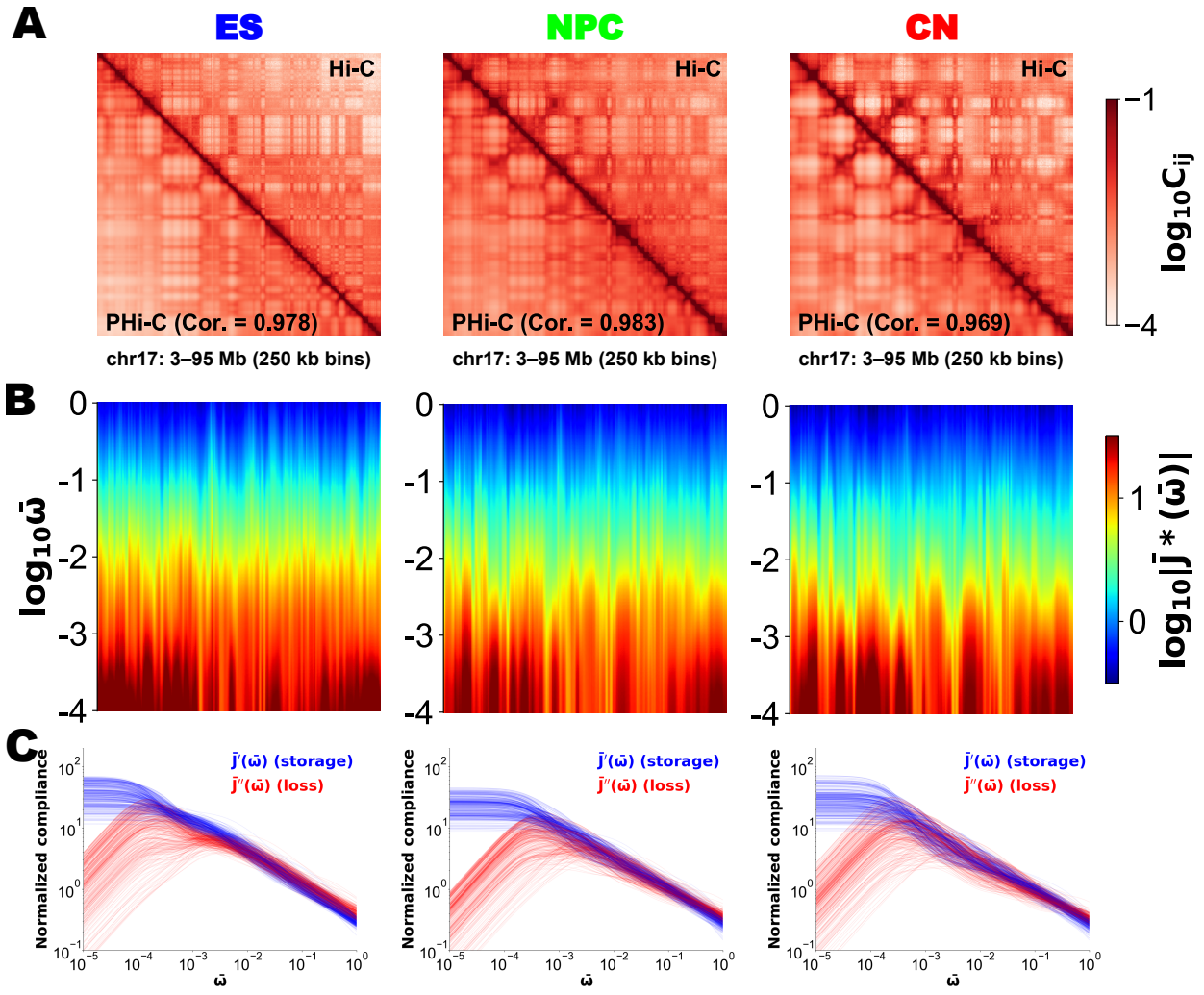

Figure S1: (A) Contact matrices for chromosome 17 during neural differentiation of mouse embryonic stem (ES) (Left), neural progenitor (NPC) (Middle), and cortical neuron (CN) (Right) cells at 250-kb resolution. Upper right and lower left elements in each matrix correspond to the normalized Hi-C contact probabilities and the optimized ones by PHi-C, respectively. (B) Spectra of the normalized complex compliance $|\bar{J}^*(\bar{\omega})|$ for chromosome 17 in ES (Left), NPC (Middle), and CN (Right) cells. Along the genomic coordinate and the logarithmic frequency $\log_{10}\bar{\omega}$, a spectrum of $|\bar{J}^*(\bar{\omega})|$ is depicted as a heat-map. (C) Frequency-dependent normalized storage (blue)

and loss (red) compliances, $\bar{J}'(\bar{\omega}; n)$ and $\bar{J}''(\bar{\omega}; n)$, for all genomic regions $n\,(= 0, 1, \cdots, 367)$ on chromosome 17 in ES (Left), NPC (Middle), and CN (Right) cells.

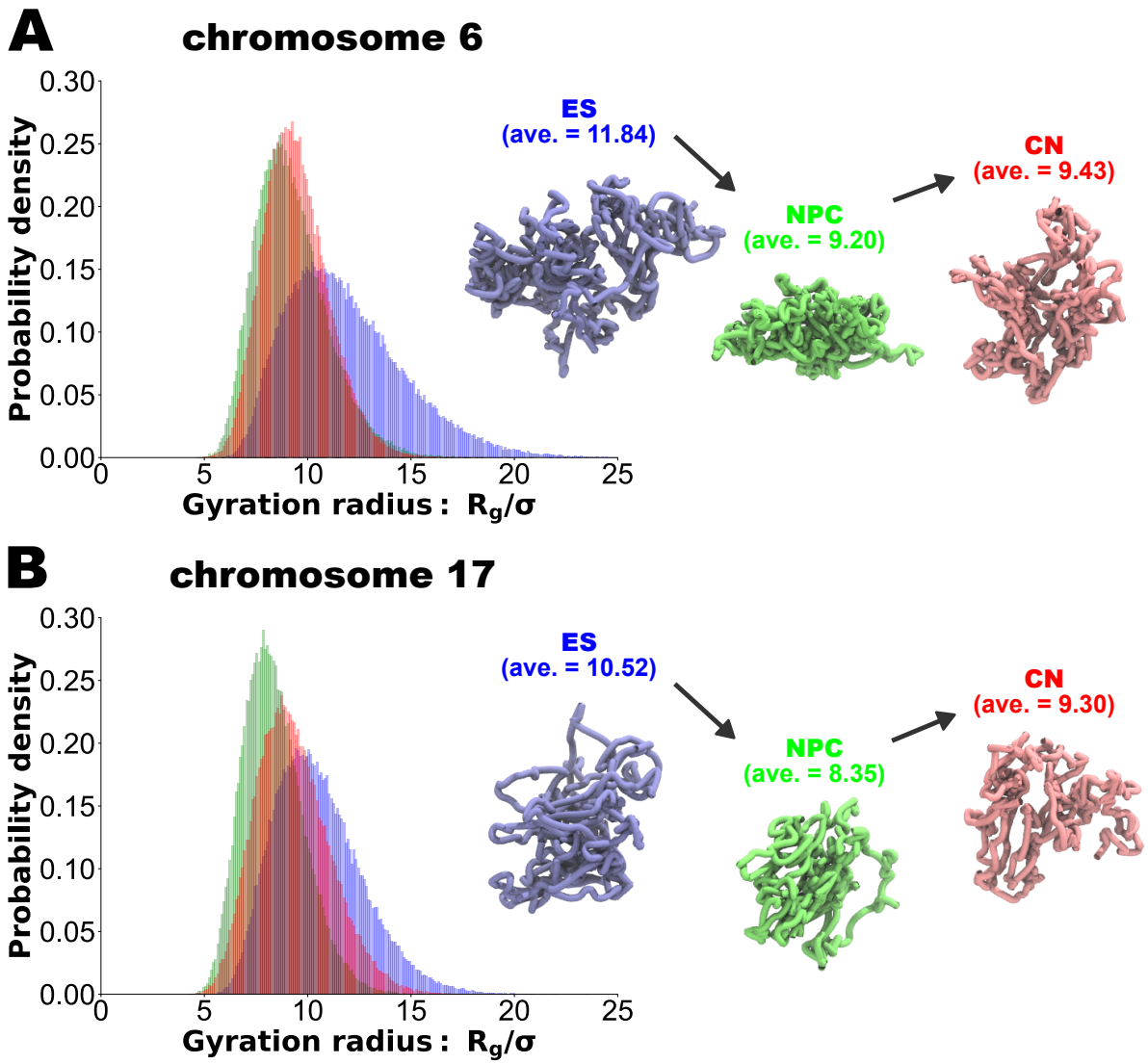

Figure S2: Probability density analysis of the normalized gyration radius $R_{\rm g}/\sigma$ of 10^5 conformations for chromosome 6 (A) and 17 (B) of mouse embryonic stem (ES; blue), neural progenitor (NPC; green), and cortical neuron (CN; red) cells. Snapshots of the polymer conformations with the average gyration radius are displayed.

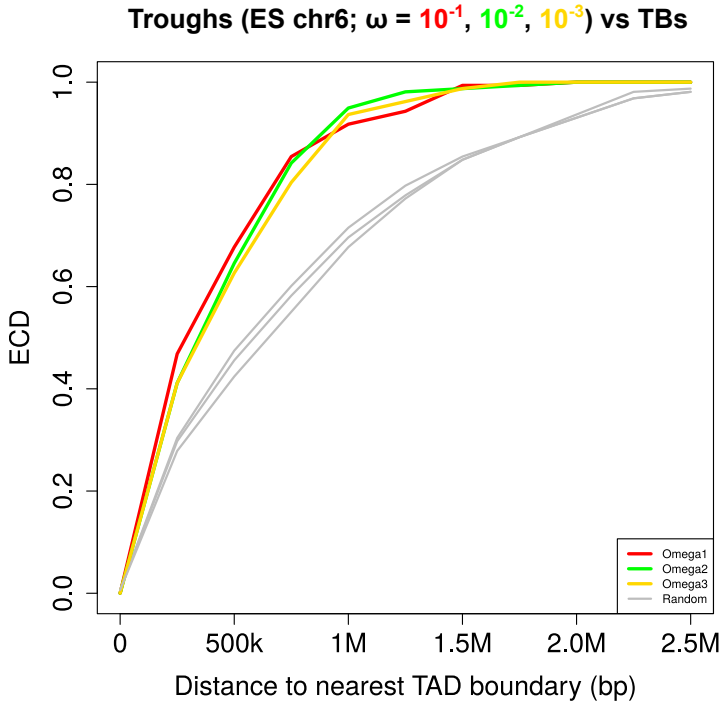

Figure S3: Cumulative probability analysis for TAD boundaries and the genomic positions of the troughs. A cumulative probability analysis of the distance between the trough positions and the nearest TAD boundaries on chromosome 6 in mouse embryonic stem (ES) cells. Red, green, gold, and grey represent the troughs from the frequency $\bar{\omega} = 10^{-1}$, 10^{-2} and 10^{-3}, and randomly permutated (control), respectively, with the former three significantly closer to the TAD boundaries than control ($p = 9.42 \times 10^{-6}$, 9.44×10^{-6}, 1.04×10^{-5}, respectively, by a two-sided Wilcoxon rank sum test). The p-values in the same analysis for chromosome 17 are also summarized on Table S1.

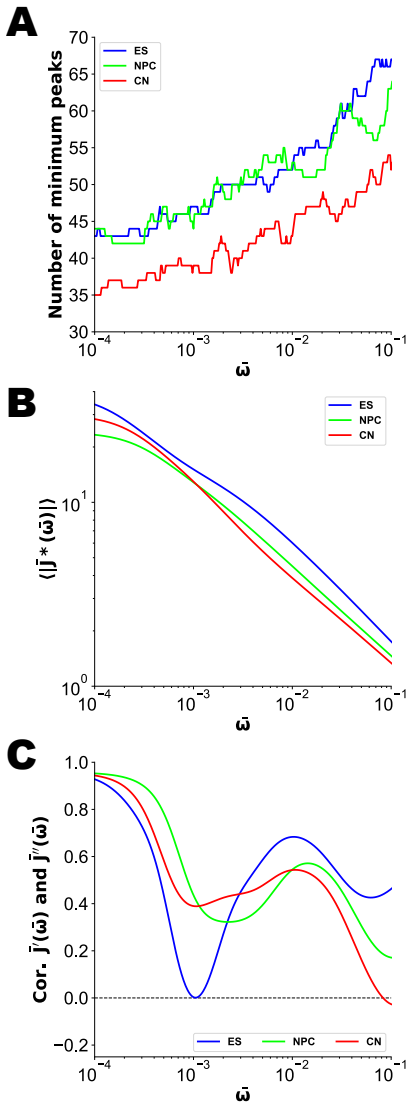

Figure S4: (A) Frequency dependence of the number of minimum peaks as the troughs on $|\bar{J}^*(\bar{\omega})|$ for chromosome 17 in mouse embryonic stem (ES), neural progenitor (NPC), and cortical neuron (CN) cells. (B) Frequency-dependent average values of $|\bar{J}^*(\bar{\omega})|$ along chromosome 17 for mouse ES, NPC, and CN cells. (C) Frequency-dependent Pearson's correlation between the normalized storage and loss compliances, $\bar{J}'(\bar{\omega})$ and $\bar{J}''(\bar{\omega})$, on chromosome 17 in mouse ES, NPC, and CN cells.

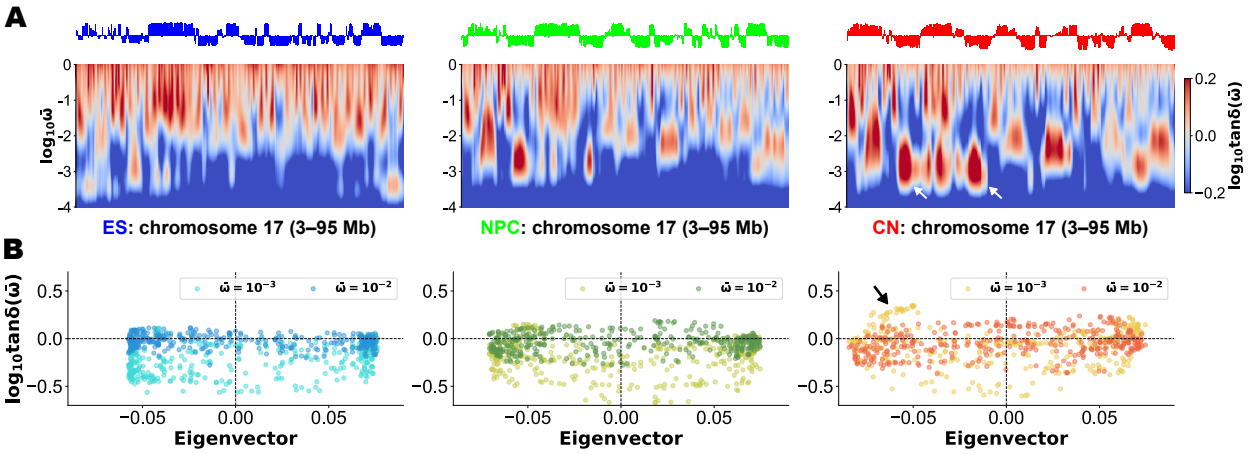

Figure S5: (A) Eigenvectors and spectra of the loss tangent $\tan\delta(\bar{\omega})$ for chromosome 17 in mouse embryonic stem (ES) (Left), neural progenitor (NPC) (Middle), and cortical neuron (CN) (Right) cells at 250-kb resolution. Along the genomic coordinate and the logarithmic frequency $\log_{10}\bar{\omega}$, a spectrum of $\tan\delta(\bar{\omega})$ is depicted as a heat-map. White arrows for CN indicate definite "island" regions around $\bar{\omega} = 10^{-3}$ with negative eigenvectors. (B) Scatter plots between the logarithmic loss tangent and the eigenvalue for $\bar{\omega} = 10^{-2}$ and $\bar{\omega} = 10^{-3}$. For CN, the black arrow indicates the appearance of the "islands" in (A).

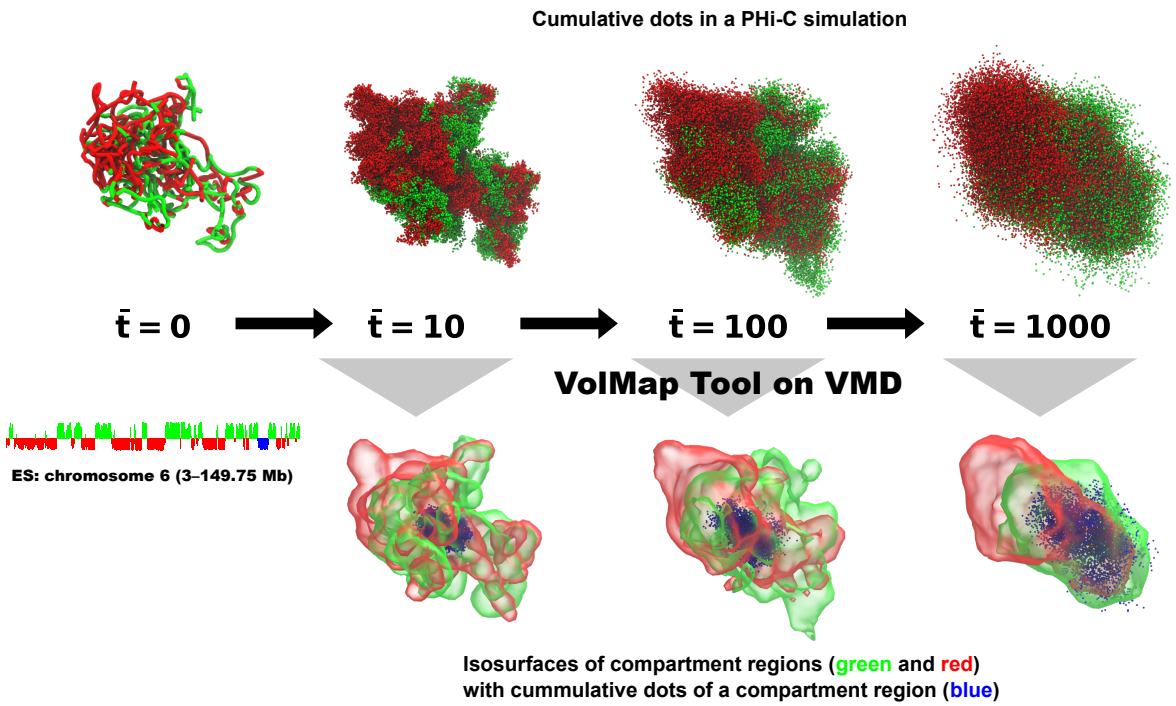

Figure S6: Isosurface plotting of compartment regions by VolMap Tool on VMD (33). According to an eigenvector profile of a Hi-C matrix, compartment regions of an initial polymer conformation at $\bar{t} = 0$ are labeled by green and red colors. A PHi-C simulation provides cumulative dots within a time interval. VolMap Tool on VMD allows for converting the labeled cumulative dots into isosurfaces of compartment regions.

Table S1: p-values by a two-sided Wilcoxon rank sum test in the cumulative probability analysis for chromosomes 6 and 17 in mouse embryonic stem (ES), neural progenitor (NPC), and cortical neuron (CN) cells.

		$\bar{\omega} = 10^{-1}$	$\bar{\omega} = 10^{-2}$	$\bar{\omega} = 10^{-3}$
chromosome 6	ES	9.42×10^{-6}	9.44×10^{-6}	1.04×10^{-5}
	NPC	2.64×10^{-5}	5.08×10^{-4}	2.60×10^{-4}
	CN	4.43×10^{-4}	9.43×10^{-4}	2.91×10^{-2}
chromosome 17	ES	3.10×10^{-5}	4.46×10^{-5}	1.87×10^{-4}
	NPC	3.18×10^{-4}	2.11×10^{-3}	1.64×10^{-2}
	CN	2.44×10^{-5}	1.87×10^{-4}	5.35×10^{-3}

Supporting Videos

Video S1: A PHi-C simulation for chromosome 6 in mouse embryonic stem cells within time $\bar{t} = 10$ regarding Fig. 3B. Here 10^4 steps of numerical integration were carried out with the normalized step time $\epsilon = 0.001$. Pink and blue dots represent the genomic positions at the peaks and troughs of $|\bar{J}^*(\bar{\omega} = 10^{-1})|$ in Fig. 3A.

Video S2: Spinning 3D structure of cumulative dots of the peaks and troughs in the simulation (Video S1) within time $\bar{t} = 10$ regarding Fig. 3B.

Video S3: Time evolution of the Cole-Cole plots between the normalized storage and loss compliances, $\bar{J}'(\bar{\omega})$ and $\bar{J}''(\bar{\omega})$, from $\bar{\omega} = 10^{-1}$ to 10^{-3} within chromosome 6 in mouse embryonic stem (Left; blue), neural progenitor (Middle; green), and cortical neuron (Right; red) cells.

Video S4: A PHi-C simulation for chromosome 6 in mouse embryonic stem cells within time $\bar{t} = 10$, which is identical to the dynamics in Video S1. According to an eigenvector profile of a Hi-C matrix, compartment regions with positive and negative eigenvectors are labeled by green and red colors, respectively.

Video S5: Spinning green- and red-labeled 3D compartments (Upper) with positive and negative eigenvectors, respectively, for chromosome 6 in mouse embryonic stem cells and the labeled cumulative dots (Lower) in the PHi-C simulation for time intervals $\bar{t} = 10$ (Left), 100 (Middle), and 1000 (Right).

Video S6: A PHi-C simulation for chromosome 6 in mouse neural progenitor cells within time $\bar{t} = 10$. Here 10^4 steps of numerical integration were carried out with the normalized step time $\epsilon = 0.001$. According to an eigenvector profile of a Hi-C matrix, compartment regions with positive and negative eigenvectors are labeled by green and red colors, respectively.

Video S7: Spinning green- and red-labeled 3D compartments (Upper) with positive and negative eigenvectors, respectively, for chromosome 6 in mouse neural progenitor cells and the labeled cumulative dots (Lower) in the PHi-C simulation for time intervals $\bar{t} = 10$ (Left), 100 (Middle), and 1000 (Right).

Video S8: A PHi-C simulation for chromosome 6 in mouse cortical neuron cells within time $\bar{t} = 10$. Here 10^4 steps of numerical integration were carried out with the normalized step time $\epsilon = 0.001$. According to an eigenvector profile of a Hi-C matrix, compartment regions with positive and negative eigenvectors are labeled by green and red colors, respectively.

Video S9: Spinning green- and red-labeled 3D compartments (Upper) with positive and negative eigenvectors, respectively, for chromosome 6 in mouse cortical neuron cells and the labeled cumulative dots (Lower) in the PHi-C simulation for time intervals $\bar{t} = 10$ (Left), 100 (Middle), and 1000 (Right).